

# Simultaneous Multislice Imaging With Slice-Multiplexed RF Pulses

K.J. Lee,\* J.M. Wild, P.D. Griffiths, and M.N.J. Paley

**A method for simultaneous multislice imaging is presented that uses a multislice RF pulse that imparts a different linear phase profile to each slice. During readout, slices are unalised by using extra slice-select gradient lobes, which rephase and dephase individual slices one at a time. Compared to other simultaneous slice methods, this method avoids distortion by slice-select gradients, and does not require extra views or additional hardware. However, because one echo per slice is required, the method requires a longer read period. This can cause non-ideal rephasing of the individual slices due to susceptibility gradients, which manifests itself as crosstalk between slices. There is also a concomitant increase in the minimum TR of the sequence. The method is demonstrated with phantom and in vivo images using gradient-echo and spin-echo versions. Magn Reson Med 54:755–760, 2005. © 2005 Wiley-Liss, Inc.**

**Key words:** simultaneous multislice MRI; rapid imaging; multiplexed pulse

If the repetition time (TR) of a scan is longer than that needed to collect data from an excited slice, one can spend this time usefully by exciting and collecting data from another interleaved slice, gradually working through the entire volume sequentially. Efficiency can be further increased by simultaneous multislice acquisitions, in which two or more slices are excited together with a single RF pulse. This is particularly useful if the required number of slices is large and several passes would be necessary for complete volume coverage (such as in thin-section imaging). In addition, simultaneity itself may be important because it provides further capabilities (e.g., the measuring blood flow velocity at multiple locations), which in turn could be used to calculate vessel compliance (and hence vessel disease) through the calculation of wave speed (1).

Current methods for simultaneous multislice imaging use a single RF pulse to excite several slices, which are then unalised during reconstruction. In the Hadamard phase cycling method termed simultaneous multislice acquisition (SIMA), the slices are encoded in a binary fashion by the RF pulse (2). The binary encoding follows a Hadamard encoding scheme, and the slices can be separated by combining them after reconstruction in a postprocessing step. For  $N$  slices,  $N$  extra views must be acquired. In another method, phase-offset multiplanar (POMP) im-

aging (3), simultaneously excited slices are given a view-dependent phase modulation. This results in different slices being shifted to non-overlapping locations in the phase-encoding direction during reconstruction. For  $N$  slices of equivalent size,  $N$  extra views are required.

Slices may also be separated in the frequency-encoding direction if the Larmor frequency of each slice is shifted by more than the imaging bandwidth. This may be accomplished by switching on the slice-select gradient during readout (4). However, the slice-select gradient distorts the slices, and if slice separation is too small, significant blurring may occur. An alternative to the slice-select gradient is to use a stepped field introduced with a  $B_0$  insert coil (5–7). In principle this avoids a slice-select gradient during readout, but the engineering requirements for high-quality steps can be very demanding, especially with small slice separations (8). If a multicoil receiver system is available, it may also be used to unalias the mixed signals, using a parallel view methodology (9).

In the proposed method, multiple slices are simultaneously excited by a single pulse (each slice has a different linear phase profile). The slices are then unalised by slice-select gradient lobe(s) in between the readout lobes.

## MATERIALS AND METHODS

A necessary requirement of the proposed method is a multislice RF pulse that imparts a different linear phase profile to each slice. The phase profiles must be such that when one slice is rephased, the other slice(s) is dephased. A simple two-slice pulse with this property may be constructed as follows: consider an asymmetrically truncated sinc-pulse (see Fig. 1a) that consists of the main lobe and one side lobe (10), and its time-reversed equivalent. Both give different linear phase profiles that require different refocusing lobes. By modulating one pulse with a linear phase modulation to shift its frequency response, before adding to the other, a simple two-slice pulse is obtained (Fig. 1b). We used the public-domain MATPULSE software to perform a Bloch simulation of the pulse (11). With rephase lobe =  $-0.30$  of slice-select gradient lobe, and flip angle =  $90^\circ$ , the excitation slice profile shown in Fig. 1c is obtained. As required, one slice is rephased while the other has a steep linear phase profile. With a rephase lobe =  $-0.75$ , the position is reversed (Fig. 1d). We found that using the composite pulse with flip angle =  $90^\circ$  gave stronger artifacts compared to those obtained with low flip angles. We surmise that this is because our pulse design was rather simplistic. For instance, due to nonlinearities, adding two pulses will not, in general, give a response that is the sum of the responses from individual pulses. In this preliminary study, we used the composite pulse with low flip angles only.

Academic Unit of Radiology, University of Sheffield, Sheffield, UK.

Grant sponsor: EPSRC; Grant number: EP/C537491/1.

\*Correspondence to: K.J. Lee, Academic Radiology, Floor C, Royal Hallamshire Hospital, Sheffield S10 2JF, UK. E-mail: k.j.lee@sheffield.ac.uk

Received 11 February 2005; revised 1 June 2005; accepted 6 June 2005.

DOI 10.1002/mrm.20643

Published online 9 September 2005 in Wiley InterScience (www.interscience.wiley.com).

© 2005 Wiley-Liss, Inc.

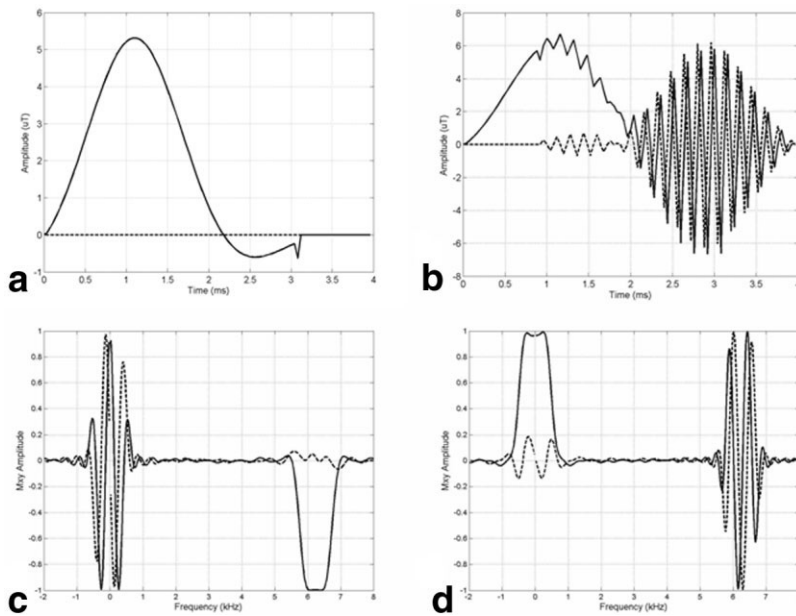


FIG. 1. Real (solid) and imaginary (dashed) (a) truncated sinc pulse and (b) composite RF pulse. Bloch simulation of pulse: excitation slice profile with rephase lobe = (c)  $-0.30$  and (d)  $-0.75$ .

### Gradient Echo

The pulse of Fig. 1b was defined at 200 points with a total duration of 4 ms. It was designed to excite two slices of 1 kHz width and 6.25 kHz separation. The pulse was used in a gradient-echo sequence with four echoes (Fig. 2). Work was performed on an Eclipse 1.5T scanner (Philips Medical Systems) with a maximum gradient strength of 27 mT/m and a rise time to maximum of 350  $\mu$ s. The first slice rephasing lobe was 0.30, and the second was 0.45 of the slice-select lobe. The third and fourth slice rephasing lobes rephase the slices once more to evaluate the effects of increased TE. The TEs from the center of the RF pulse were 5.3, 7.6, 9.9, and 12.2 ms. The extra read gradient lobe at the end serves as a spoiler to suppress transverse coherence at short TR. Phantom data were acquired from a structured doped water phantom with flip angle =  $25^\circ$ , TR = 200 ms, field of view (FOV) = 30 cm, number of averages (NSA) = 1, sampling bandwidth (BW) = 125 kHz, and matrix size =  $256 \times 128$  (read  $\times$  phase). Slice thickness was varied between 2 and 5 mm to assess the effects of susceptibility gradients. Axial brain images were acquired from a normal volunteer with TR = 400 ms, FOV = 30 cm, matrix size =  $256 \times 256$ , slice thickness = 2 mm, BW = 125 kHz, and NSA = 2.

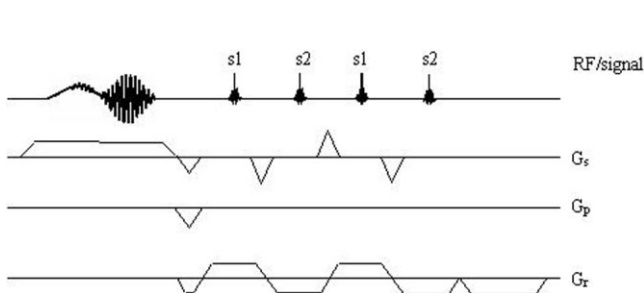


FIG. 2. Gradient-echo sequence diagram. The slice multiplexed RF pulse is followed by slice gradient lobes that rephase and dephase the slices sequentially. The final read gradient lobe dephases residual transverse magnetization. TE = 5.3, 7.6, 9.9, and 12.2 ms.

### Spin Echo

The same truncated sinc pulses were also used in a spin-echo sequence (Fig. 3) on the same scanner, but modulated to select slices at  $\pm 12.5$  kHz. The dual-slice RF refocusing pulse was constructed by modulating a  $180^\circ$  RF pulse to have the same frequency response as the excitation pulse. This rather crude refocusing pulse was used to demonstrate proof of principle, and experiments showed that in order to minimize crosstalk between slices, the slice rephasing lobes must be 33% and 63% of the slice-select lobe, rather than the 30% and 75% used for gradient echoes. The TEs were chosen to be 30, 33, 98.4, and 101.4 ms, so that images from the first spin echo are predominantly proton-density weighted, and those from the second are predominantly  $T_2$  weighted. Phantom data were acquired from a water phantom with flip angle =  $25^\circ$ , TR = 400 ms, slice thickness = 2 mm, FOV = 30 cm, matrix size =  $256 \times 256$ , BW = 125 kHz, and NSA = 2. Axial brain images were acquired from a normal volunteer with flip angle =  $25^\circ$ , TR = 1500 ms, slice thickness = 2 mm, FOV = 30 cm, matrix size =  $256 \times 256$ , BW = 125 kHz, and NSA = 3.

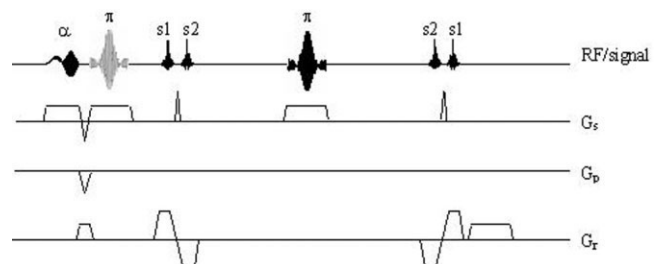
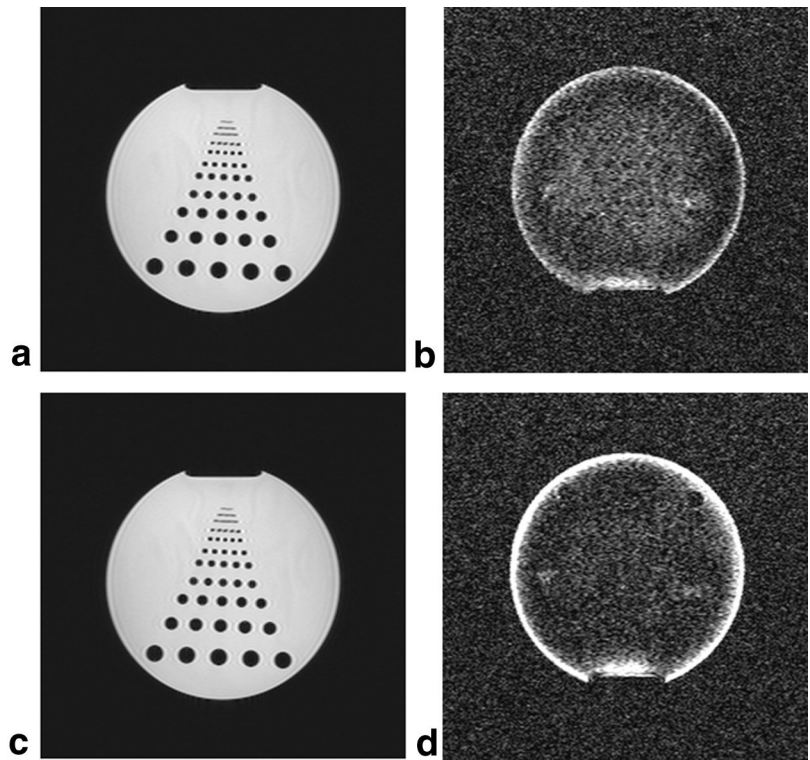


FIG. 3. Spin-echo sequence diagram. Two refocusing pulses follow the slice multiplexed pulse, forming spin echoes. On either side of each spin echo there is a gradient-recalled echo. Each echo contains signal predominantly from the rephased slice. TE = 30, 33, 98, and 101 ms. The final read gradient lobe serves to suppress coherence artifacts at short TR.

FIG. 4. Gradient-echo phantom images at TE = (a) 5.3, (b) 7.6, (c) 9.9, and (d) 12.2 ms. One of the slices was positioned in air to show crosstalk between slices. At later TEs, crosstalk signal is stronger at the phantom edge where susceptibility gradients are strong. Note that b and d have been rewindowed to enhance low signal, which would otherwise have been practically invisible.



**RESULTS**

Gradient Echo

Figure 4a–d show phantom images obtained from echoes 1–4 (slices in order: s1, s2, s1, s2), with one of the slices

positioned in air to show crosstalk between slices. Slice thickness was 5 mm. Ghost intensity was measured to be approximately 1% of the phantom image. It can be seen that intensity is increased around the edge of the phantom at longer TE, as might be expected from the superposition

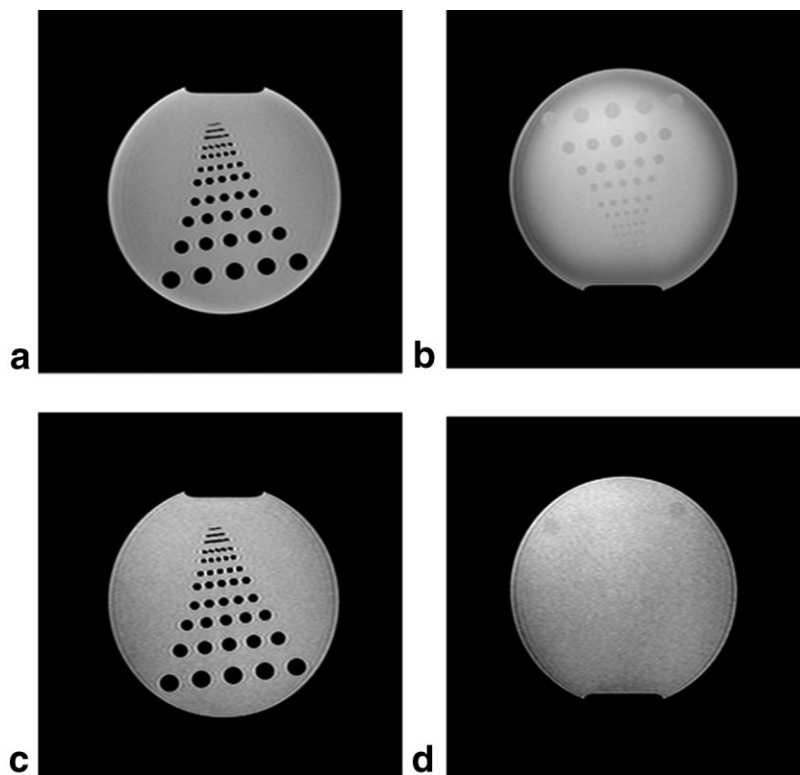


FIG. 5. Gradient-echo phantom images. Left images: TE = 9.9 ms. Right images: TE = 12.2 ms. Top row images are from 5-mm-thick slices, and lower row images are from 2-mm-thick slices. Against a uniform background, crosstalk from the other slice is prominent. This is reduced by reducing the slice thickness. Note that d has been rewindowed to enhance the contrast of the low-level artifact.

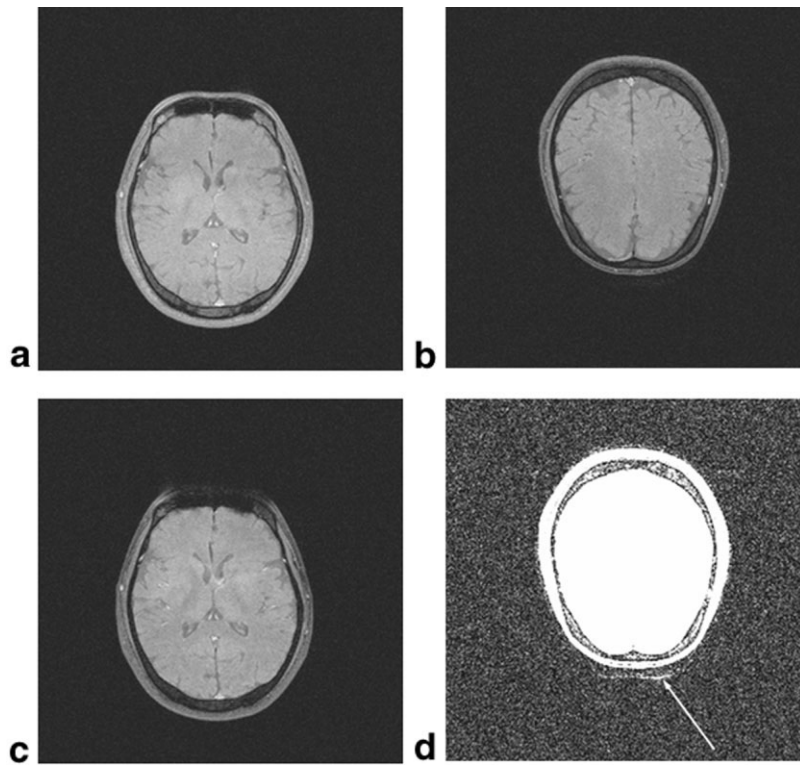


FIG. 6. Gradient-echo axial brain images. TE = (a) 5.3, (b) 7.6, (c) 9.9, and (d) 12.2 ms. In c there is signal loss around the sinus. Some of this signal appears in the other slice, most clearly in the later echo image (see arrow). Image d has been rewinded to highlight the crosstalk artifact.

of susceptibility gradients causing incomplete dephasing. Figure 5 shows phantom images with both slices in the phantom. Slice thickness is 5 mm in Fig. 5a and b, and crosstalk is clearly visible against the uniform background. To reduce the incomplete dephasing caused by susceptibility gradients, a thinner slice thickness = 2 mm was

chosen and the corresponding images show almost no crosstalk (Fig. 5c and d).

In brain images (Fig. 6), the inferior slice was positioned over the frontal sinus. At the later TE, signal loss due to susceptibility gradients around the sinus can be seen (Fig. 6c). Some signal leakage around this area is

FIG. 7. Spin-echo phantom images with 2-mm-thick slices at TE = (a) 30, (b) 33, (c) 98.4, and (d) 101.4 ms. Some crosstalk due to susceptibility differences is visible (arrows). Image c has been rewindowed to show the crosstalk more clearly. Without rewinding, the artifact appearance was similar to that in part b.

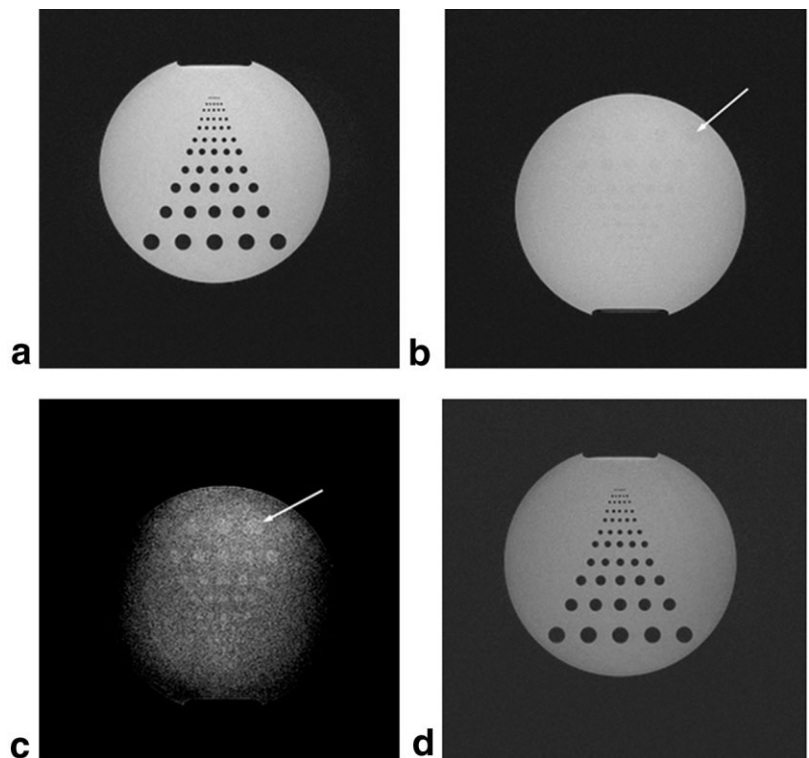
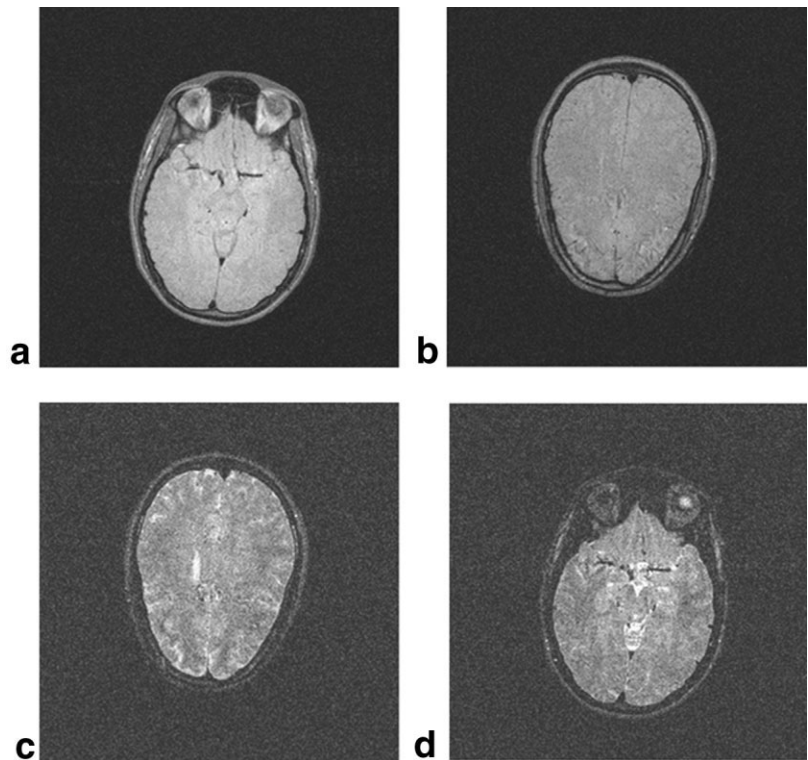


FIG. 8. Spin-echo axial brain images. TE = (a) 30, (b) 33, (c) 98.4, and (d) 101.4 ms. Images a and b are predominantly proton-density weighted, while c and d are predominantly  $T_2$ -weighted. Images c and d have been brightened to compensate for  $T_2$  signal loss.



visible in Fig. 6d. However, there is no other sign of crosstalk.

### Spin Echo

Figure 7a–d show phantom images obtained from echoes 1–4 (in order s1, s2, s2, s1). The gradient echoes were positioned symmetrically around the spin echo, and some crosstalk is visible. However, axial brain images using the same sequence show predominantly proton- and  $T_2$ -weighted images, respectively, with no visible crosstalk (Fig. 8).

### DISCUSSION

At the heart of the method is a pulse that multiplexes multiple slices by giving each slice a different linear phase profile: when one slice is rephased by the slice gradient, the others are dephased. The success of the method depends on reducing crosstalk between slices. The degree of dephasing is entirely dependent on the phase “twist” across a slice; therefore, crosstalk will be greatest where there is incomplete dephasing caused by superposition of in-slice background gradients due to susceptibility differences (12), and our results confirm this. In our phantom studies, crosstalk was most apparent at the air/water interfaces. In the gradient-echo brain images, there was crosstalk at the frontal sinus (Fig. 6). Reducing susceptibility artifacts (e.g., by reducing slice thickness or TE) will also improve the method, as demonstrated by Fig. 5. It is not possible to rephase susceptibility gradients completely in all slices even with the spin-echo sequence, as Fig. 7 demonstrates. However, the in vivo brain images with the same sequence show that the artifacts were at an acceptable level (Fig. 8).

The spin-echo sequence is similar to the gradient- and spin-echo (GRASE) sequence, with gradient reversals in between RF refocusing pulses (13). In our method each echo gives a  $k$ -space line in a different slice, unlike GRASE, where each echo gives another  $k$ -space line within the same slice. Compared to GRASE, we might expect fewer artifacts due to  $k$ -space inconsistencies, but at a cost of some susceptibility crosstalk, and higher-power refocusing pulses.

It might be argued that our method is not, strictly speaking, simultaneous. Although the RF pulse is a single composite, it has two lobes corresponding to different slices, and therefore one slice experiences the bulk of its excitation at a slightly different time from that of another slice, albeit with a difference that is less than the duration of a single noncomposite pulse. Furthermore, from consideration of the Fourier shift theorem, it can be seen that increased phase difference is achievable only with increased lobe separation. In the limit of total separation, there are two pulses, each of which excites one slice, followed by a single phase-encode and readout period. Therefore, this proposed method can be viewed as intermediate between methods that excite multiple slices truly simultaneously with one pulse (2–7,9), and methods that rapidly excite multiple slices with sequential pulses but share a single phase-encode and readout interval, such as multislice interleaved excitation cycles (MUSIC) (14) and simultaneous echo refocusing (SER) (15). Consequently, our method has improved simultaneity compared to MUSIC and SER, but does not require the extra views or hardware used in truly simultaneous slice methods.

In future work we hope to improve the RF pulse design for both gradient- and spin-echo sequences to reduce slice

ripple, improve phase profiles, and excite more slices. Incorporating pulse nonlinearities by designing with the Shinnar-Le Roux algorithm (16) will enable higher flip angles and better SNR.

## ACKNOWLEDGMENT

K.J. Lee was supported by an EPSRC First Grant Scheme award (EP/C537491/1).

## REFERENCES

- Dumoulin CL, Doorly DJ, Caro CG. Quantitative measurement of velocity at multiple positions using comb excitation and Fourier velocity encoding. *Magn Reson Med* 1993;29:44–52.
- Souza SP, Szumowski J, Dumoulin CL, Plewes DP, Glover G. SIMA: simultaneous multislice acquisition of MR images by Hadamard-encoded excitation. *J Comput Assist Tomogr* 1988;12:1026–1030.
- Glover GH. Phase-offset multiplanar (POMP) volume imaging: a new technique. *J Magn Reson Imaging* 1991;1:457–461.
- Weaver JB. Simultaneous multislice acquisition of MR images. *Magn Reson Med* 1988;8:275–284.
- Paley MN, Lee KJ, Wild JM, Fische S, Whitby EH, Wilkinson ID, van Beek EJ, Griffiths PD. B1AC-MAMBA: B1 array combined with multiple-acquisition micro B0 array parallel magnetic resonance imaging. *Magn Reson Med* 2003;49:1196–1200.
- Lee KJ, Paley MN, Wilkinson ID, Griffiths PD. Magnetic resonance imaging with stepped B-0 fields. *Magn Reson Imaging* 2003;21:625–629.
- Paley MNJ, Lee KJ, Wild JM, Whitby EH, Griffiths PD. Interleaved pulsed MAMBA: a new parallel slice imaging method. *Magn Reson Med* 2002;48:1043–1050.
- Lee KJ, Paley MNJ, Barber DC, Wilkinson ID, Griffiths PD. Target field design for MAMBA step fields. *Concepts Magn Reson Part B* 2004;20B:1–8.
- Larkman DJ, Hajnal JV, Herlihy AH, Coutts GA, Young IR, Ehnholm G. Use of multicoil arrays for separation of signal from multiple slices simultaneously excited. *J Magn Reson Imaging* 2001;13:313–317.
- McKinnon GC. On self-refocusing pulses for rapid gradient-echo imaging. *Magn Reson Med* 1993;29:260–262.
- Matson GB. An integrated program for amplitude-modulated RF pulse generation and re-mapping with shaped gradients. *Magn Reson Imaging* 1994;12:1205–1225.
- Wild JM, Martin WR, Allen PS. Multiple gradient echo sequence optimized for rapid, single-scan mapping of  $R(2)^*$  at high B0. *Magn Reson Med* 2002;48:867–876.
- Oshio K, Feinberg DA. GRASE (gradient- and spin-echo) imaging: a novel fast MRI technique. *Magn Reson Med* 1991;20:344–349.
- Loenneker T, Hennel F, Hennig J. Multislice interleaved excitation cycles (MUSIC): an efficient gradient-echo technique for functional MRI. *Magn Reson Med* 1996;35:870–874.
- Feinberg DA, Reese TG, Wedeen VJ. Simultaneous echo refocusing in EPI. *Magn Reson Med* 2002;48:1–5.
- Pauly J, Leroux P, Nishimura D, Macovski A. Parameter relations for the Shinnar-Leroux selective excitation pulse design algorithm. *IEEE Trans Med Imaging* 1991;10:53–65.